Sodium selenate mitigates tau pathology, neurodegeneration, and functional deficits in Alzheimer's disease models

Janet van Eersel[a,b], Yazi D. Ke[a], Xin Liu[a], Fabien Delerue[a], Jillian J. Kril[b], Jürgen Götz[a,1], and Lars M. Ittner[a,1]

[a]Alzheimer's and Parkinson's Disease Laboratory, Brain and Mind Research Institute, University of Sydney, Camperdown, New South Wales 2050, Australia; and [b]Department of Pathology, University of Sydney, Camperdown, New South Wales 2016, Australia

Communicated by Etienne-Emile Baulieu, Institut National de la Sante et de la Recherche Médicale, Le Kremlin-Bicetre, France, June 25, 2010 (received for review June 7, 2010)

Alzheimer's disease (AD) brains are characterized by amyloid-β-containing plaques and hyperphosphorylated tau-containing neurofibrillary tangles (NFTs); however, in frontotemporal dementia, the tau pathology manifests in the absence of overt amyloid-β plaques. Therapeutic strategies so far have primarily been targeting amyloid-β, although those targeting tau are only slowly beginning to emerge. Here, we identify sodium selenate as a compound that reduces tau phosphorylation both in vitro and in vivo. Importantly, chronic oral treatment of two independent tau transgenic mouse strains with NFT pathology, P301L mutant pR5 and K369I mutant K3 mice, reduces tau hyperphosphorylation and completely abrogates NFT formation. Furthermore, treatment improves contextual memory and motor performance, and prevents neurodegeneration. As hyperphosphorylation of tau precedes NFT formation, the effect of selenate on tau phosphorylation was assessed in more detail, a process regulated by both kinases and phosphatases. A major phosphatase implicated in tau dephosphorylation is the serine/threonine-specific protein phosphatase 2A (PP2A) that is reduced in both levels and activity in the AD brain. We found that selenate stabilizes PP2A-tau complexes. Moreover, there was an absence of therapeutic effects in sodium selenate-treated tau transgenic mice that coexpress a dominant-negative mutant form of PP2A, suggesting a mediating role for PP2A. Taken together, sodium selenate mitigates tau pathology in several AD models, making it a promising lead compound for tau-targeted treatments of AD and related dementias.

frontotemporal lobar degeneration | protein phosphatase 2A | neurofibrillary tangle | transgenic | treatment

Alzheimer's disease (AD) is the most prevalent neurodegenerative disorder, characterized by progressive loss of cognition. Histopathologically, AD is defined by two lesions, plaques and neurofibrillary tangles (NFTs), which result from deposition of amyloid-β (Aβ) and hyperphosphorylated tau, respectively. Aβ forms upon cleavage of the amyloid precursor protein by β- and γ-secretases, and accumulates extracellularly (1). Tau accumulates intracellularly as it becomes increasingly phosphorylated at both physiological and pathological sites, resulting in reduced affinity to microtubules and redistribution from the axonal to the somato-dendritic compartment (2). The amyloid cascade hypothesis places Aβ upstream of tau, a concept supported by AD mouse models (3, 4). Interestingly, tau depletion in mice prevents Aβ pathology, suggesting that Aβ toxicity is also tau-dependent (5). This finding highlights a central pathogenic role of tau in AD. This role extends to diseases such as frontotemporal dementia, the second most common form of dementia, where tau lesions are frequent without overt Aβ pathology (2). Thus, tau can induce neurodegeneration in the absence of Aβ. Accordingly, expression of tau in transgenic mouse models recapitulates features of AD and frontotemporal lobar degeneration (FTLD) (6).

Selenium is a vital trace element enriched in brain (7, 8); its levels decline with age, and particularly low levels have been linked to cognitive impairment and AD (9, 10). Short-term administration of selenium improves memory deficits in an acute rat model of dementia (11) and reduces tau phosphorylation in WT rats (12). Therefore, selenium has been attributed neuroprotective properties, but the underlying mechanism and its therapeutic potential remain elusive (11).

To date, treatment of AD and related dementias is limited to symptomatic relief, with no cure available. Although Aβ has been the main focus of drug development until recently, tau is increasingly recognized as a target for the treatment of AD and FTLD (13). Here, we tested putative therapeutic effects of sodium selenate, an oxidized form of selenium, on tau pathology, using cell culture and several transgenic mouse models.

Results

Sodium Selenate Reduces Tau Phosphorylation in Vitro. To test selenate in vitro, we first treated SH-SY5Y neuroblastoma cells that stably express human tau carrying the FTLD pathogenic mutation P301L (SH-P301L). In these cells, tau is phosphorylated at multiple sites, including the pathological epitope Ser422 (pS422), a site correlating with NFT formation in vivo (3, 14) (Fig. 1 *A* and *B*). Selenate treatment reduced pS422 staining without affecting tau expression levels (Fig. 1 *A* and *B*, and Fig. S1). Western blotting of extracts obtained from both selenate-treated and untreated cells in the presence of the protein phosphatase 2A (PP2A) inhibitor okadaic acid (OA) revealed a dose-dependent reduction of tau phosphorylation at multiple sites, including pS422, 12E8, and PHF-1 (Fig. 1 *C*).

Toxicity has been reported for some forms of selenium, such as sodium selenite (15), which would severely compromise a therapeutic use. We thus assessed neurotoxicity of sodium selenate compared with selenite, a less oxidized state of selenium, by measuring lactate dehydrogenase (LDH) release in primary hippocampal cultures (Fig. 1 *D*). Although selenite was toxic already at low concentrations, selenate showed no toxicity, even at high 100 μM concentrations. Furthermore, chronic treatment of mice with selenate over 4 mo did not cause any overt side effects or any form of neurotoxicity (see below).

Selenate Improves Tau Transgenic K3 Mice. Given the profound effects on tau phosphorylation in vitro, we next tested if selenate also reduces hyperphosphorylation of tau in vivo. K3 mice express human tau carrying the pathogenic K369I mutation in neurons (16). These neurons are characterized by a particularly early-onset

Author contributions: J.v.E., J.G., and L.M.I. designed research; J.v.E., Y.D.K., X.L., F.D., and L.M.I. performed research; J.v.E., Y.D.K., X.L., F.D., J.G., and L.M.I. analyzed data; and J.v.E., J.J.K., J.G., and L.M.I. wrote the paper.

The authors declare no conflict of interest.

[1]To whom correspondence may be addressed. E-mail: jgoetz@med.usyd.edu.au or littner@med.usyd.edu.au.

This article contains supporting information online at www.pnas.org/lookup/suppl/doi:10.1073/pnas.1009038107/-/DCSupplemental.

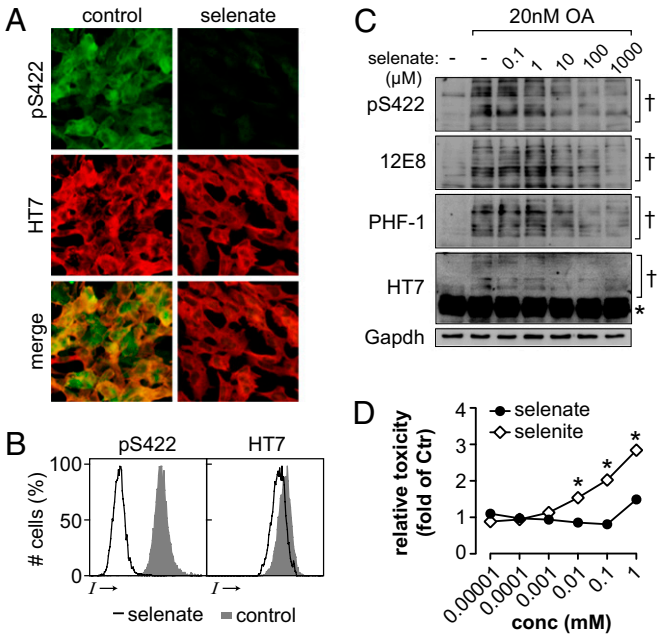

Fig. 1. Sodium selenate mitigates aberrant tau phosphorylation in SH-SY5Y neuroblastoma cells. (*A*) Immunocytochemistry of human P301L mutant tau expressing SH-SY5Y cells treated with selenate. Phosphorylation of tau at the pathological epitope Ser422 (pS422) is markedly reduced in selenate-treated cells, although total tau (HT7) is comparable to untreated controls. (*B*) Flow cytometry confirms reduced pS422 phosphorylation, but similar HT7 staining upon selenate treatment, compared with control. *I*, fluorescence intensity. (*C*) OA induces phosphorylation of tau at multiple epitopes (pS422, 12E8, PHF-1), resulting in a molecular weight shift (†) in SH-SY5Y cells. Cotreatment with increasing doses of selenate shows a dose-dependent reduction of tau phosphorylation, but levels of nonphosphorylated tau (asterisk) remain unaltered. (*D*) Dose-dependent increase in toxicity of selenite, but not selenate in primary hippocampal neurons, as determined by LDH release (*$P < 0.001$).

Parkinsonism associated with abundant tau phosphorylation, and axonal transport defects (16, 17). We first treated 6-wk-old K3 mice with 12 μg/mL selenate added to the drinking water ad libitum, with controls receiving no drug, and monitored the progression of motor symptoms. Selenate did not affect total water consumption (Fig. S2). K3 mice normally exhibit motor deficits on the Rota-Rod already at 6 wk, compared with WT (Fig. 2*A*). However, although untreated K3 mice (further) declined dramatically over time until they failed to stay on the rod at all, selenate-treated K3 mice showed a gradually improving motor performance, such that after 6 wk of treatment they were no longer distinguishable from WT littermates. The motor improvement was associated with decreased tau phosphorylation in the motor cortex, hippocampus, and substantia nigra (Fig. 2*B* and Fig. S3). Staining of brain sections for tau phosphorylated at Thr231/Ser235 (AT180 epitope), a major phosphorylation site in K3 mice (16), revealed significantly reduced phosphorylation in selenate- compared with untreated mice. Importantly, transgenic *tau* mRNA levels were not altered upon treatment (Fig. S1). Hence, selenate reduces both tau phosphorylation and early-onset motor deficits in young K3 mice.

Tau pathology in K3 mice is progressive. Beyond the age of 4 mo, deposition of tau results in overt Bielschowsky-silver-positive NFT-like inclusions and axonal spheroids in many brain areas, as well as in neurodegeneration in the substantia nigra (16, 17). When we treated 4-mo-old K3 mice until 8 mo of age with selenate, numbers of inclusions were significantly reduced, as shown for the hippocampal subiculum and midbrain (Fig. 2 *C–E*). Furthermore, numbers of spheroids, a result of axonal transport defects in K3 mice (17), were significantly lower in treated mice (Fig. 2*F*). In fact, spheroids were completely absent from frontal cortex, suggesting that selenate reverts functional impairments leading to spheroids. K3 mice are characterized by a substantial, age-dependent degeneration of cerebellar basket neurons, resulting in the absence of pinceau terminals formed by clustered axons surrounding Purkinje cells (Fig. 2*G*). Selenate treatment fully prevented this degeneration. Taken together, these findings show that selenate reduces tau phosphorylation and deposition, mitigates pathological spheroid formation, and prevents axonal degeneration of distinct neuronal populations in K3 mice.

Selenate Halts Pathology in Tau Transgenic pR5 Mice. Next, we treated 8-mo-old pR5 mice that express P301L mutant human tau in neurons (18) for 4 mo with 12 μg/mL selenate added to the drinking water. The pR5 mice present with a progressive tau pathology, including NFT formation initiated at around 6 mo of age (18). These mice are characterized by an amygdala-dependent impairment in the conditioned taste aversion (CTA) paradigm (19). As expected, untreated pR5 mice displayed a significant impairment, although selenate-treated pR5 mice showed no impairment, performing similar to wild-type littermates and hence, suggestive of improved contextual memory (Fig. 3*A*). Basic taste qualities were normal in untreated and treated pR5 mice (Fig. S2). Next, we determined whether the functional improvement of selenate-treated pR5 mice was associated with changes in tau pathology. Double-staining for human tau (HT7) and tau phosphorylated at Ser422 (pS422) revealed reduced phosphorylation in CA1 neurons of selenate-treated compared with untreated pR5 mice, although staining for total tau was comparable (Fig. 3*B*). As for the K3 mice, transgenic *tau* mRNA levels were not altered by selenate (Fig. S1). Next, we determined if selenate treatment reduces levels of insoluble tau, a step critical in NFT formation. Therefore, we extracted pR5 brain tissue with either formic acid (FA) or sarkosyl to obtain insoluble proteins (16, 20). Consistent with the histopathological finding, Western blotting revealed reduced phosphorylation of tau in selenate-treated pR5 brains, although total levels of soluble tau were comparable in treated and untreated pR5 mice (Fig. 3 *C* and *D*). However, both FA and sarkosyl extraction revealed markedly less insoluble tau in selenate-treated compared with untreated pR5 mice. The amygdala is a major site of NFT formation in pR5 mice (18). Here, both numbers of neurons stained with pS422, a marker of severe tau pathology (3), and numbers of Gallyas-positive NFTs were significantly reduced in selenate-treated compared with untreated pR5 brains (Fig. 3 *E* and *F*). Specifically, NFT numbers in 12-mo-old selenate-treated pR5 mice were similar to those in 8-mo-old untreated pR5 mice (3), suggesting that treatment had halted disease progression.

Selenate-Induced Improvements Require PP2A. Reduced PP2A activity has been implicated in AD (21, 22). Because selenate antagonized the PP2A inhibitor OA in SH-SY5Y cells (Fig. 1*C*), we addressed PP2A function in more detail. Regulation of tau phosphorylation by PP2A involves direct binding (23). Interestingly, coimmunoprecipitation of PP2A from SH-SY5Y cells with a tau-specific antibody revealed a markedly increased tau-PP2A interaction in the presence of increasing doses of selenate (Fig. 4*A* and Fig. S4), suggesting that selenate enhances tau binding of PP2A.

To determine the role of PP2A in mediating the effects of selenate on tau pathology in vivo, we crossed pR5 with Dom5 mice (pR5.Dom5). Dom5 mice express a substrate-specific dominant-negative mutant form of PP2A, L309A (24). The two transgenes show an overlapping expression pattern in pR5.Dom5 mice, including the hippocampus (25). Although selenate treatment of pR5 mice reduced levels of tau phosphorylation significantly, treatment had no effect in pR5.Dom5 mice, as determined by Western blot analysis of hippocampal extracts (Figs. 2*C* and 4*B*

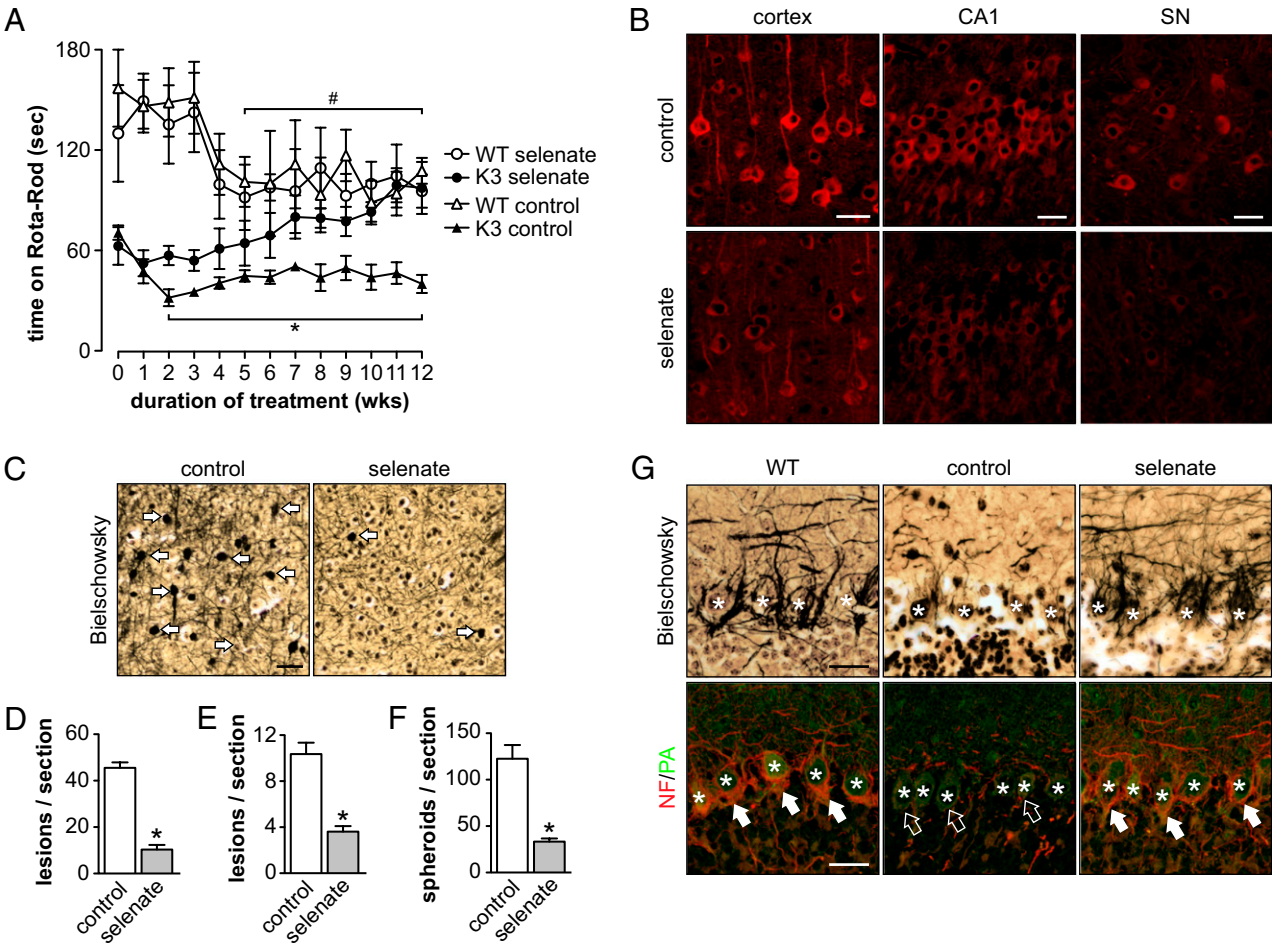

Fig. 2. Chronic selenate treatment improves pathology in both young and aged K369I mutant tau transgenic K3 mice. (*A*) Rota-Rod testing in acceleration mode of selenate-treated and untreated (control) WT and K3 mice. Despite pronounced deficits in K3 compared with WT mice at the onset of treatment (6 wk of age), after 5 wk of chronic selenate treatment motor performance of K3 mice is improved such that performance does not differ significantly from WT ($^{\#}$n.s.), although untreated K3 control mice continue to deteriorate, staying only for a minimal time on the rod (*$P < 0.05$, treated vs. untreated K3 mice). (*B*) Selenate treatment for 12 wk significantly reduces staining of K3 brains with the phospho-tau antibody AT180 (Thr231/Ser235), a dominant phospho-epitope in K3 mice, in neurons of cortex, hippocampal CA1, and substantia nigra (SN), compared with untreated K3 mice (for quantification, see Fig. S3). (Scale bars, 50 μm.) (*C*) Bielschowsky-silver positive NFT-like lesions (arrows) are numerous in the superior colliculus of the midbrain of 8-mo-old untreated K3 mice (control), but are significantly reduced after 4 mo of treatment with selenate. (Scale bar, 50 μm.) (*D*) Quantification reveals that numbers of lesions are 4.4-fold lower in the superior colliculus of selenate-treated compared with untreated (control) K3 mice (*$P < 0.0001$). (*E*) Numbers of NFT-like lesions in the subiculum are 2.87-fold lower in selenate-treated compared with untreated (control) K3 mice (*$P < 0.0001$). (*F*) Axonal spheroids are 3.68-fold less frequent in the cortex of selenate-treated compared with untreated (control) K3 mice (*$P < 0.0001$). (*G*) Bundled axons of cerebellar basket cell form Pinceau terminals (arrows) around the initial axon segment of the Purkinje cell (PC, asterisks), as visualized by Bielschowsky-silver impregnation and neurofilament (NF) staining (red) in WT brains. Eight-month-old untreated K3 mice (control) show a pronounced degeneration of Pinceau terminals, resulting in the absence of NF- and Bielschowsky-positive axons around PCs (open arrows). Treatment with selenate fully prevents this degeneration. PCs are stained with parvalbumin (PA, green). (Scale bar, 50 μm.)

and Fig. S4). Furthermore, extraction of insoluble proteins revealed high levels of insoluble tau in selenate-treated pR5.Dom5, but not pR5 mice. Consistent with these findings, the histological analysis revealed that selenate had no effect on preventing tau phosphorylation and NFT formation in pR5.Dom5 mice (Fig. 4 *C* and *D*). Therefore, the absence of therapeutic effects in pR5.Dom5 mice suggests a role for PP2A in the selenate-induced reduction of tau phosphorylation.

Increased kinase activities have been implicated in AD (26). Although selenate may alter kinase function, Western blot analysis of wild-type and K3 brains with phosphorylation (activity)- and total kinase-specific antibodies (GSK3β, ERK1/2, p38 Mapk, and cdk5) revealed no alterations upon chronic selenate treatment (Fig. S5). Therefore, altered kinase activity seems not to contribute to the effects of selenate on tau phosphorylation.

Discussion

In the present study, we show that chronic low doses of sodium selenate reduce tau phosphorylation in both cell culture and mouse models of disease. Treatment prevents memory and motor deficits, NFT formation, and degeneration in two tau transgenic mouse lines with robust pathologies. These effects are, at least in part, mediated by PP2A, because selenate does not reduce tau phosphorylation in mice coexpressing a defective PP2A subunit (which causes reduced activity for substrates such as tau).

PP2A is a heterotrimeric complex composed of a structural A, a catalytic C, and a variable regulatory B subunit (27). Four classes of regulatory subunits, B (PR55), B' (B56 or PR61), B" (PR72), and B"' (PR93/PR110), with several members in each subfamily, define substrate specificity and subcellular localization of the holoenzyme. This result is also true for the PP2A substrate tau

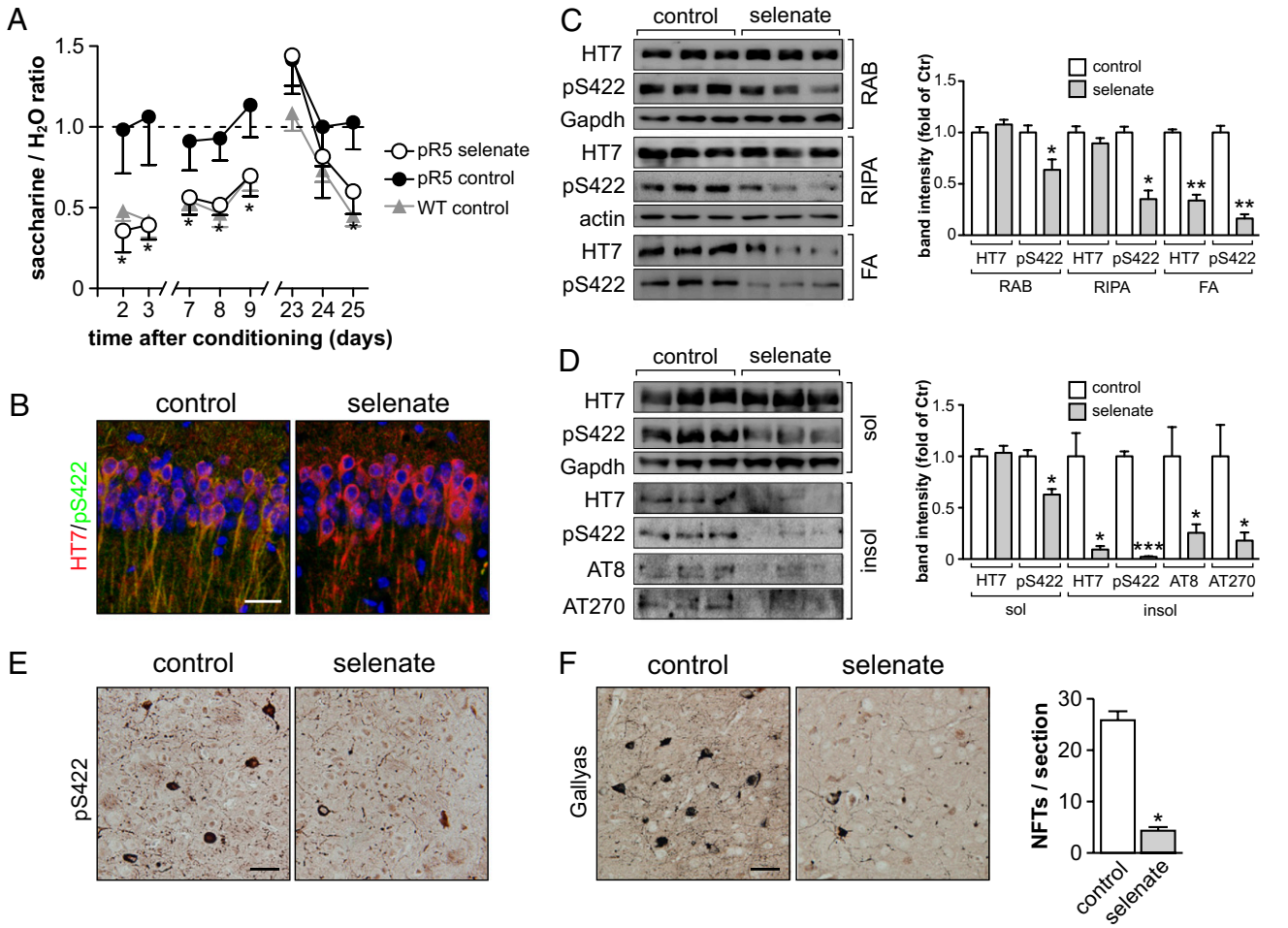

Fig. 3. Chronic selenate treatment improves the phenotype of P301L mutant tau transgenic pR5 mice. (*A*) Amygdala-dependent CTA is impaired in untreated (control) 12-month-old pR5 mice, as indicated by equal saccharine and water consumption; WT mice remember the nausea associated with saccharine consumption during conditioning and hence, consume less saccharine. Treatment of pR5 mice with selenate for 4 mo reverts CTA to WT levels (*$P < 0.05$ vs. pR5 control/WT). (*B*) Immunohistochemistry (IHC) for human tau (HT7, red) and phospho-tau (pS422, green) shows pS422 staining only in pR5 control CA1 neurons (yellow merge), although HT7 staining is similar in control and selenate-treated pR5. (Scale bar, 50 μm.) (*C*) Extraction of brain tissue with buffers of increasing stringency shows reduction of both tau phosphorylation (pS422) and levels of insoluble human tau (HT7, FA fraction) in selenate-treated compared with control pR5 mice. Total levels of soluble human tau, extracted in salt- (RAB), and detergent-containing (RIPA) buffers, are similar in control and selenate-treated pR5 brains. Gapdh and actin show loading. Quantified band intensities are presented as fold of control (*$P < 0.05$; **$P < 0.001$). (*D*) Similarly, extraction of sarkosyl-soluble (sol) and -insoluble (insol) proteins shows a significant reduction in tau phosphorylation at multiple sites (pS422, AT8, AT270) and levels of insoluble human tau (HT7). Gapdh shows loading. Quantified band intensities are presented as fold-changes of control (*$P < 0.05$; ***$P < 0.0001$). (*E*) IHC with pS422 stains numerous neurons in control pR5 amygdala, but rarely in selenate-treated pR5 brains. (Scale bar, 50 μm.) (*F*) Accordingly, numbers of Gallyas-silver positive NFTs are 6.04-fold reduced in selenate-treated compared with control pR5 brains (*, $P < 0.001$). (Scale bar, 50 μm.)

that is dephosphorylated, upon binding, by distinct isoforms of PP2A (23, 28). Interestingly, we found that selenate increases binding of PP2A and tau in cell culture, which may explain its effects on tau phosphorylation. Other mechanisms of regulating PP2A activity may include alterations in the methylation of the core enzyme or dislodging of catalytic metal atoms (29, 30). Here, the exact molecular effects of selenate on PP2A and other likely, yet unidentified cellular targets remain to be elucidated. However, given the role proposed for PP2A in tau pathology in AD (21, 22, 28, 31), activating PP2A represents an attractive therapeutic approach (26). It should be considered, however, that interfering with the activity of PP2A may cause side effects, as the holoenzyme participates in several signaling cascades in many tissues other than brain. Hence, a substrate-specific activation of PP2A rather than a broad inhibition needs to be achieved. Although in K3 and pR5 mice, tau phosphorylation was reduced in the absence of overt central or peripheral side effects, it cannot formally be ruled out that other pathways are also affected, which may lead to side effects during long-term treatment in humans.

In the past, targeting Aβ pathology has been the major avenue pursued in developing treatments for AD (32, 33). However, tau is increasingly appreciated as a drug target (13). Importantly, targeting tau extends treatment to tau-only dementias, of which there are many. Current strategies in developing tau-directed treatments include inhibition of tau aggregation (34–38), stabilization of microtubules (39, 40), inhibition of kinases (41, 42), induction of tau clearance (43–45), immunotherapy (46), and indirect modulation of tau function (47). So far, however, only a limited number of compounds proved efficacy in tau transgenic mouse models, and even fewer progressed into clinical trials (13). Many compounds are limited with respect to bioavailability, blood–brain barrier permeability and specificity, and are accompanied by severe systemic side effects. Therefore, it is promising that chronic treatment with low doses of selenate results in reduced hyperphosphorylation and deposition of tau, together with improved memory and prevention of neurodegeneration in vivo. Importantly, these effects occur in the absence of obvious side effects. Hence, our data recommend selenate as a lead compound for drug development in human disease.

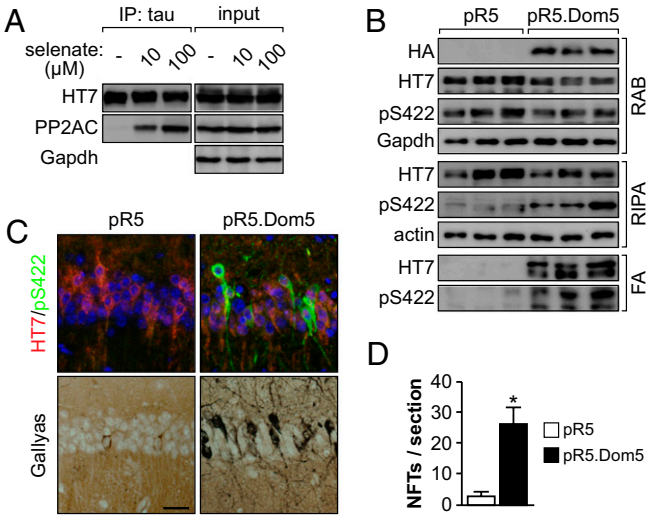

Fig. 4. Role for PP2A in mediating the therapeutic effects of selenate. (*A*) Coimmunoprecipitation of tau from SH-SY5Y cells reveals a markedly increased pull-down of the PP2A catalytic subunit upon selenate treatment, compared with untreated cells (for quantification, see Fig. S4). (*B*) Dom5 mice express an HA-tagged dominant-negative mutant form of the catalytic subunit of PP2A (L309A) in neurons. The pR5 mice were crossed with Dom5 mice (pR5.Dom5), treated with selenate at 9 mo of age (for 4 mo), and analyzed at 13 mo of age. Extraction of brain tissue with buffers of increasing stringency shows significantly increased levels of tau phosphorylation (pS422) and insoluble human tau (HT7) in the FA fraction of selenate-treated pR5.Dom5 compared with selenate-treated pR5 mice. Total levels of soluble human tau are similar in selenate-treated pR5 and pR5.Dom5 brains, as determined by extraction in high salt- (RAB) and detergent-containing (RIPA) buffers (for quantification, see Fig. S4). Gapdh and actin show loading. (*C*) CA1 neurons show little phospho-tau (pS422) reactivity in selenate-treated pR5, and staining is pronounced in selenate-treated pR5.Dom5 brains. Total human tau (HT7) staining is, however, comparable. Gallyas silver-positive NFTs, although rare in the hippocampus of selenate-treated pR5 mice, are abundant in treated pR5.Dom5 mice. (Scale bar, 50 μm.) (*D*) Quantification of serial sections reveals 11.86-fold more NFTs in pR5.Dom5 compared with pR5 mice upon selenate treatment (*$P < 0.001$).

Methods

Mice. The K3, pR5, and Dom5 strains have been previously described (16, 18, 24). Hemizygous pR5 and Dom5 mice were crossed to establish pR5.Dom5 double-transgenic mice, and single-transgenic pR5 littermates were used as controls. Six-week-old K3 mice were treated with sodium selenate (Sigma) for 3 mo, and 4-mo-old K3, 8-mo-old pR5, and 9-mo-old pR5.Dom5 and control littermates were treated for 4 mo. Six to eight mice were used per experimental group. Anesthetized mice were transcardially perfused with PBS (Sigma), brains harvested, and hemispheres separated. One hemisphere was subdissected and frozen for biochemical analysis, and the other hemisphere was immersion-fixed in 4% paraformaldehyde (PFA, Sigma) before being processed for histological analysis. The animal experiments were approved by the Animal Ethics Committee of the University of Sydney.

Cell Culture. Human SH-SY5Y neuroblastoma cells were cultured in DMEM/F-12 medium (Gibco) supplemented with 10% FBS (Invitrogen), L-glutamine, and penicillin/streptomycin (Invitrogen) at 37 °C/5% CO_2. For culturing SH-SY5Y cells that stably express P301L mutant human tau (SH-P301L) (14), 125 μg/mL of gentamycin (Invitrogen) was added to the medium. Primary hippocampal neurons were cultured for 20 d, as previously described (48). Cells were treated with (sodium) selenate and selenite (Sigma) at the indicated concentrations for 12 h. Toxicity in primary neurons was determined using the cytotoxicity detection kit PLUS (Roche) that measures LDH release.

Flow Cytometry. Cells were harvested using trypsin/EDTA (Gibco), washed in PBS, and fixed with 4% PFA. Cells were permeabilized with 1% saponin (Sigma) for 20 min, blocked with FACS buffer (PBS/1%FBS) for 1 h, and incubated with primary antibodies to human tau (HT7; Thermo) and tau phosphorylated at Ser422 (pS422; Invitrogen) overnight at 4 °C. Alexa-coupled secondary antibodies (Molecular Probes) were used for detection. Cells from three independent experiments were run on an LSR-II (BD Biosciences) flow cytometer and data were analyzed with the FlowJo8.8.4 software (Tree Star).

Western Blotting. Proteins were extracted according to solubility as described, using FA or sarkosyl (49, 50). Western blotting was performed as described (51). Primary antibodies were to human tau (HT7), tau phosphorylated at S422 (pS422; Invitrogen), S262/S356 (12E8; P. Seubert, Elan Pharmaceuticals, San Francisco, CA), S396/S404 (PHF-1; P. Davies, Albert Einstein College of Medicine, New York, NY), S202/T205 (AT8) and T181 (AT270; Thermo), PP2A subunit C (PP2AC; Millipore), Gapdh and actin (both Chemicon), and HA tag (Roche). Blots were detected and quantified in a VersaDoc 4000 system (BioRad).

Immunocytochemistry. Fixed cells were stained as previously described (51). Primary antibodies pS422 and HT7 were visualized with Alexa-coupled secondary antibodies. Digital images were taken with a BX51 fluorescence microscope (Olympus).

Immunoprecipitation. Immunoprecipitation (IP) was performed as described (17), using a tau-specific antibody produced in rabbit (Dako) for coprecipitation of PP2A in IP buffer (50 mM Tris-HCl (pH8.0), 150 mM NaCl, 1% Nonidet P-40 substitute (all Sigma), and complete, EDTA-free protease inhibitor mixture (1 tablet in 40 mL; Roche). Antibodies were pulled-down with magnetic Dynabeads Protein G (Invitrogen) and washed four times with IP buffer before eluting with sample buffer for SDS/PAGE.

Histology. PFA-fixed brains were embedded in paraffin using an Excalibur tissue processor (Thermo). Immunohistochemistry was done as described (52). Antigen retrieval was done in a temperature- and pressure-controlled microwave system (Milestone) in Tris/EDTA pH9.0 for 7 min at 120 °C, followed by cooling under running tap water for 10 min. Primary antibodies were HT7, pS422, AT180 (tau phosphorylated at T231/S235), 200kD neurofilament (NF; Abcam) and parvalbumin (PA; Abcam). Alexa- or biotin-coupled secondary antibodies were used for detection, together with the ABC-HRP detection kit (Vector) using metal enhanced DAB (Pierce). Counterstaining was done with hematoxylin (HD Scientific) or DAPI (Molecular Probes). Bielschowsky- and Gallyas-silver impregnation of paraffin sections was done as described (16). Fluorescence intensity was quantified on serial sagittal sections ($n = 6$) with ImageJ (National Institutes of Health) using the measure function. NFTs were counted on serial sections, as described previously (3).

Motor and Behavioral Testing. Motor performance of K3 and wild-type mice was tested on a five-wheel Rota-Rod treadmill (Ugo Basile) in acceleration mode (5–60 rpm) over 120 s using a 180-s cutoff time. The longest time each mouse remained on the turning wheel out of five attempts per session was counted. The CTA paradigm was carried out as described (19).

Luciferase Reporter Assay. Tau promoter reporter cells were generated by lentiviral gene transfer of the previously identified tau promoter sequence (53) cloned upstream of a firefly luciferase (*luc2P*; Promega) encoding cDNA into SH-SY5Y cells. Promoter activity was measured after incubation with Bright-Glo Luciferase Assay substrate (Promega) in a FLUOstar Omega luminescence plate reader (BMG Labtech).

Quantitative PCR. RNA was isolated from cells or brain tissue with TRIzol (Invitrogen) according to the manufacturer's instructions and treated with RQ1 DNase (Promega) to remove any contaminating genomic DNA. Complementary DNA was synthesized from mRNA using AffinityScript multiple temperature reverse transcriptase (Stratagene) for 90 min at 50 °C. Quantitative PCR was performed in an Mx3000p cycler (Stratagene) using SYBR green (Roche) and the following primers: tau forward (5′-TAGCTGACGAGGTGTCTGCC-3′), tau reverse (5′-ATTTGAAGGACTTGGGGAGG-3′), Gapdh forward (5′-AGGTCGGTGTGAACGGATTTG-3′) and Gapdh reverse (5′-TGTAGACCATGTAGTTGAGGTC-3′). Ct values for tau were normalized to those of Gapdh.

Statistical Testing. Statistical analysis was done with Prism 5.0 (GraphPad). All values are given as mean ± SE.

ACKNOWLEDGMENTS. We thank Dr. Nikolas Haass for help with FACS experiments and Drs. Peter Seubert and Peter Davies for antibodies. This work has been supported by the University of Sydney, the National Health and Medical Research Council, the Australian Research Council, Diabetes Australia Research Trust, and the J. O. and J. R. Wicking Trust. Postgraduate scholarship support has been provided by the Australian Government, the Wenkart Foundation, GlaxoSmithKline, and Alzheimer's Australia.

1. Haass C, Selkoe DJ (2007) Soluble protein oligomers in neurodegeneration: Lessons from the Alzheimer's amyloid beta-peptide. *Nat Rev Mol Cell Biol* 8:101–112.
2. Ballatore C, Lee VM, Trojanowski JQ (2007) Tau-mediated neurodegeneration in Alzheimer's disease and related disorders. *Nat Rev Neurosci* 8:663–672.
3. Götz J, Chen F, van Dorpe J, Nitsch RM (2001) Formation of neurofibrillary tangles in P301l tau transgenic mice induced by Abeta 42 fibrils. *Science* 293:1491–1495.
4. Lewis J, et al. (2001) Enhanced neurofibrillary degeneration in transgenic mice expressing mutant tau and APP. *Science* 293:1487–1491.
5. Roberson ED, et al. (2007) Reducing endogenous tau ameliorates amyloid beta-induced deficits in an Alzheimer's disease mouse model. *Science* 316:750–754.
6. Götz J, Ittner LM (2008) Animal models of Alzheimer's disease and frontotemporal dementia. *Nat Rev Neurosci* 9:532–544.
7. Rayman MP (2000) The importance of selenium to human health. *Lancet* 356:233–241.
8. Benton D (2002) Selenium intake, mood and other aspects of psychological functioning. *Nutr Neurosci* 5:363–374.
9. Akbaraly TN, et al. (2007) Plasma selenium over time and cognitive decline in the elderly. *Epidemiology* 18:52–58.
10. Cardoso BR, et al. (2010) Nutritional status of selenium in Alzheimer's disease patients. *Br J Nutr* 103:803–806.
11. Ishrat T, et al. (2009) Selenium prevents cognitive decline and oxidative damage in rat model of streptozotocin-induced experimental dementia of Alzheimer's type. *Brain Res* 1281:117–127.
12. Yim SY, et al. (2009) ERK activation induced by selenium treatment significantly down-regulates beta/gamma-secretase activity and Tau phosphorylation in the transgenic rat overexpressing human selenoprotein M. *Int J Mol Med* 24:91–96.
13. Brunden KR, Trojanowski JQ, Lee VM (2009) Advances in tau-focused drug discovery for Alzheimer's disease and related tauopathies. *Nat Rev Drug Discov* 8:783–793.
14. Ferrari A, Hoerndli F, Baechi T, Nitsch RM, Götz J (2003) Beta-Amyloid induces paired helical filament-like tau filaments in tissue culture. *J Biol Chem* 278:40162–40168.
15. Nuttall KL (2006) Evaluating selenium poisoning. *Ann Clin Lab Sci* 36:409–420.
16. Ittner LM, et al. (2008) Parkinsonism and impaired axonal transport in a mouse model of frontotemporal dementia. *Proc Natl Acad Sci USA* 105:15997–16002.
17. Ittner LM, Ke YD, Götz J (2009) Phosphorylated Tau interacts with c-Jun N-terminal kinase-interacting protein 1 (JIP1) in Alzheimer disease. *J Biol Chem* 284:20909–20916.
18. Götz J, Chen F, Barmettler R, Nitsch RM (2001) Tau filament formation in transgenic mice expressing P301L tau. *J Biol Chem* 276:529–534.
19. Pennanen L, Welzl H, D'Adamo P, Nitsch RM, Götz J (2004) Accelerated extinction of conditioned taste aversion in P301L tau transgenic mice. *Neurobiol Dis* 15:500–509.
20. Goedert M, Spillantini MG, Cairns NJ, Crowther RA (1992) Tau proteins of Alzheimer paired helical filaments: abnormal phosphorylation of all six brain isoforms. *Neuron* 8:159–168.
21. Gong CX, et al. (1995) Phosphatase activity toward abnormally phosphorylated tau: Decrease in Alzheimer disease brain. *J Neurochem* 65:732–738.
22. Vogelsberg-Ragaglia V, Schuck T, Trojanowski JQ, Lee VM (2001) PP2A mRNA expression is quantitatively decreased in Alzheimer's disease hippocampus. *Exp Neurol* 168: 402–412.
23. Sontag E, et al. (1999) Molecular interactions among protein phosphatase 2A, tau, and microtubules. Implications for the regulation of tau phosphorylation and the development of tauopathies. *J Biol Chem* 274:25490–25498.
24. Schild A, Ittner LM, Götz J (2006) Altered phosphorylation of cytoskeletal proteins in mutant protein phosphatase 2A transgenic mice. *Biochem Biophys Res Commun* 343: 1171–1178.
25. Deters N, Ittner LM, Götz J (2009) Substrate-specific reduction of PP2A activity exaggerates tau pathology. *Biochem Biophys Res Commun* 379:400–405.
26. Gong CX, Iqbal K (2008) Hyperphosphorylation of microtubule-associated protein tau: A promising therapeutic target for Alzheimer disease. *Curr Med Chem* 15:2321–2328.
27. Janssens V, Goris J (2001) Protein phosphatase 2A: A highly regulated family of serine/threonine phosphatases implicated in cell growth and signalling. *Biochem J* 353: 417–439.
28. Sontag E, Nunbhakdi-Craig V, Lee G, Bloom GS, Mumby MC (1996) Regulation of the phosphorylation state and microtubule-binding activity of Tau by protein phosphatase 2A. *Neuron* 17:1201–1207.
29. Xing Y, et al. (2008) Structural mechanism of demethylation and inactivation of protein phosphatase 2A. *Cell* 133:154–163.
30. Wu J, et al. (2000) Carboxyl methylation of the phosphoprotein phosphatase 2A catalytic subunit promotes its functional association with regulatory subunits in vivo. *EMBO J* 19:5672–5681.
31. Liu F, Grundke-Iqbal I, Iqbal K, Gong CX (2005) Contributions of protein phosphatases PP1, PP2A, PP2B and PP5 to the regulation of tau phosphorylation. *Eur J Neurosci* 22: 1942–1950.
32. Hardy J, Selkoe DJ (2002) The amyloid hypothesis of Alzheimer's disease: Progress and problems on the road to therapeutics. *Science* 297:353–356.
33. Selkoe DJ, Schenk D (2003) Alzheimer's disease: Molecular understanding predicts amyloid-based therapeutics. *Annu Rev Pharmacol Toxicol* 43:545–584.
34. Wischik CM, Edwards PC, Lai RY, Roth M, Harrington CR (1996) Selective inhibition of Alzheimer disease-like tau aggregation by phenothiazines. *Proc Natl Acad Sci USA* 93: 11213–11218.
35. Chirita C, Necula M, Kuret J (2004) Ligand-dependent inhibition and reversal of tau filament formation. *Biochemistry* 43:2879–2887.
36. Pickhardt M, et al. (2007) Phenylthiazolyl-hydrazide and its derivatives are potent inhibitors of tau aggregation and toxicity in vitro and in cells. *Biochemistry* 46: 10016–10023.
37. Taniguchi S, et al. (2005) Inhibition of heparin-induced tau filament formation by phenothiazines, polyphenols, and porphyrins. *J Biol Chem* 280:7614–7623.
38. Crowe A, et al. (2009) Identification of aminothienopyridazine inhibitors of tau assembly by quantitative high-throughput screening. *Biochemistry* 48:7732–7745.
39. Zhang B, et al. (2005) Microtubule-binding drugs offset tau sequestration by stabilizing microtubules and reversing fast axonal transport deficits in a tauopathy model. *Proc Natl Acad Sci USA* 102:227–231.
40. Matsuoka Y, et al. (2008) A neuronal microtubule-interacting agent, NAPVSIPQ, reduces tau pathology and enhances cognitive function in a mouse model of Alzheimer's disease. *J Pharmacol Exp Ther* 325:146–153.
41. Pérez M, Hernández F, Lim F, Díaz-Nido J, Avila J (2003) Chronic lithium treatment decreases mutant tau protein aggregation in a transgenic mouse model. *J Alzheimers Dis* 5:301–308.
42. Le Corre S, et al. (2006) An inhibitor of tau hyperphosphorylation prevents severe motor impairments in tau transgenic mice. *Proc Natl Acad Sci USA* 103:9673–9678.
43. Dickey CA, et al. (2007) The high-affinity HSP90-CHIP complex recognizes and selectively degrades phosphorylated tau client proteins. *J Clin Invest* 117:648–658.
44. Luo W, et al. (2007) Roles of heat-shock protein 90 in maintaining and facilitating the neurodegenerative phenotype in tauopathies. *Proc Natl Acad Sci USA* 104:9511–9516.
45. Berger Z, et al. (2006) Rapamycin alleviates toxicity of different aggregate-prone proteins. *Hum Mol Genet* 15:433–442.
46. Asuni AA, Boutajangout A, Quartermain D, Sigurdsson EM (2007) Immunotherapy targeting pathological tau conformers in a tangle mouse model reduces brain pathology with associated functional improvements. *J Neurosci* 27:9115–9129.
47. Chambraud B, et al. (2010) A role for FKBP52 in Tau protein function. *Proc Natl Acad Sci USA* 107:2658–2663.
48. Fath T, Ke YD, Gunning P, Götz J, Ittner LM (2009) Primary support cultures of hippocampal and substantia nigra neurons. *Nat Protoc* 4:78–85.
49. Ke YD, Delerue F, Gladbach A, Götz J, Ittner LM (2009) Experimental diabetes mellitus exacerbates tau pathology in a transgenic mouse model of Alzheimer's disease. *PLoS ONE* 4:e7917.
50. van Eersel J, et al. (2009) Phosphorylation of soluble tau differs in Pick's disease and Alzheimer's disease brains. *J Neural Transm* 116:1243–1251.
51. Ittner LM, Koller D, Muff R, Fischer JA, Born W (2005) The N-terminal extracellular domain 23-60 of the calcitonin receptor-like receptor in chimeras with the parathyroid hormone receptor mediates association with receptor activity-modifying protein 1. *Biochemistry* 44:5749–5754.
52. Ittner LM, et al. (2005) Compound developmental eye disorders following inactivation of TGFbeta signaling in neural-crest stem cells. *J Biol* 4:11.
53. Sadot E, Heicklen-Klein A, Barg J, Lazarovici P, Ginzburg I (1996) Identification of a tau promoter region mediating tissue-specific-regulated expression in PC12 cells. *J Mol Biol* 256:805–812.